ASEAN Journal of Chemical Engineering 2022, Vol. 22, No. 2, 284 – 295

A Comparative Study on The Electrochemical Properties of Hydrothermal and Solid-State Methods in The NCM Synthesis for Lithium Ion Battery Application

***Sylvia Ayu Pradanawati*[1]**
***Eduardus Budi Nursanto*[2]**
***Afif Thufail*[3]**
***Ahmad Zaky Raihan*[3]**
***Sugianto*[3]**
***Haryo Satriya Oktaviano*[4]**
***Hanida Nilasary*[4]**
***Achmad Subhan*[5]**
***Agung Nugroho**,[2]**

[1]*Department of Mechanical Engineering, Universitas Pertamina, Jalan Teuku Nyak Arief, Simprug, Kebayoran Lama, Jakarta 12220, Indonesia.*
[2]*Department of Chemical Engineering, Universitas Pertamina, Jalan Teuku Nyak Arief, Simprug, Kebayoran Lama, Jakarta 12220, Indonesia.*
[3]*Department of Chemistry, Universitas Pertamina, Jalan Teuku Nyak Arief, Simprug, Kebayoran Lama, Jakarta 12220, Indonesia.*
[4]*Downstream Research and Technology Innovation, Research and Technology Innovation, PT Pertamina (Persero), Sopo Del Tower A, Floor 51, Jakarta 12950, Indonesia.*
[5]*Research Center for Advanced Materials-National Research and Innovation Agency, Tangerang Selatan 15314, Indonesia*
*e-mail: agung.n@universitaspertamina.ac.id

Submitted 19 April 2022 *Revised* 24 September 2022 *Accepted* 6 October 2022

Abstract. In this article, we report and compare the synthesis method of the active cathode materials based on nickel - cobalt - manganese (NCM) for lithium-ion battery application. We evaluate the hydrothermal and solid-state reaction method in NCM-622 synthesis, the material characterizations, and the battery performance. Based on the analytical results using X-ray diffraction (XRD), particles synthesized using hydrothermal and solid-state methods exhibit a highly crystalline NCM phase. NCM particles synthesized using solid-state reaction exhibit high-rate performance up to 10 C. The electrochemical impedance spectroscopy analysis shows that the charge transfer resistance (Rct) of NCM synthesized by the solid-state reaction (SSR) method was 25.9% lower than hydrothermal. Meanwhile, the ionic diffusivity of the SSR sample was 38.5% higher than the hydrothermal sample. These two factors lead to better performance when tested in a lithium-ion battery.

Keywords: Battery Performance, Lithium Ion Battery, NCM, Synthesis

DOI: 10.22146/ajche.74209

INTRODUCTION

Since the past decade, electric vehicle demand has been increasing worldwide, which is dominated by battery electric vehicles (BEVs) (Andre et al., 2015). The evolution of applications of BEVs vehicle began with hybrid vehicles (HVs) to plug-in hybrids (PHEVs) and became fully electric vehicles (EVs). In BEVs, Lithium-Ion Batteries (LIBs) are the most battery used for energy storage due to their large capacity, high energy density, high specific power, and long life cycle. LIBs have three main parts in their system: cathode, anode, and electrolyte, which can affect the electrochemical properties of LIBs. However, the major obstacle of LIBs on BEVs is the field of cathode materials because it has a lower capacity than anode materials. To achieve better performances, efficiency, and energy conversion of LIBs, cathode materials play a crucial role (Andre et al., 2015, Geldasa et al., 2022, Julien et al., 2014, Or et al., 2020, Park et al., 2011).

The first cathode material to be commercialized was Lithium Cobalt Oxide (LCO) in 1991 by Sony. However, these materials still have a problem with high toxicity levels and high costs. The theoretical capacity of the LCO is 270 mAh/g at a potential of 4.2 V vs. Li/Li^+ (Andre et al., 2015). Nevertheless, the practical capacity is only about 140 mAh/g, and only 0.5 mol Li^+ is utilized to prevent the transition metal dissolution and electrolyte oxidation during the cycle (Andre et al., 2015, Or et al., 2020). To overcome this issue, several cathode materials have been developed, such as Lithium Iron Phosphate ($LiFePO_4$, LFP), Lithium Manganese Oxide ($LiMn_2O_4$, LMO), Lithium Nickel Cobalt Aluminium Oxides ($LiNiCoAlO_2$, NCA), and Lithium Nickel Manganese Cobalt Oxide ($LiNiCoMnO_2$, NCM) (Geldasa et al., 2022, Julien et al., 2014, Park et al., 2011).

The NCM has been widely used as a cathode in lithium-ion batteries in the full cell arrangement. The specific capacity value of these materials when applied as full cells of LIB is 150-220 mAh/g at 0.1 C (Li et al., 2020, Seungbum et al., 2022, Wu et al., 2019). Nickel-rich cathode material is one of the alternatives cathodes of LIBs based on NCM to be applied for EVs because of the high energy density, strong charge-discharge capacity, and thermal stability in a typical layered structure (Liu et al., 2014, Myung et al., 2017).

In NCM, high nickel content contributes to higher capacity performance. Meanwhile, cobalt and manganese content contributes to an increased lifetime and stability in cycle performance (Bak et al., 2014, Kim, 2012, Konishi et al., 2013, 2011, Wu et al., 2011). Therefore, NCM with nickel-rich content can be used as an alternative promising cathode material.

The metal compositions of NCM configuration that have been developed are 111, 523, 622, and 811, where each configuration has various electrochemical characteristics (Deng et al., 2010, Jan et al., 2014, Konishi et al., 2013, Liu et al., 2014, Myung et al., 2017, Wang et al., 2016, Zheng et al., 2015). Based on electrochemical performances (capacity, lifetime, and stability), efficiency, and energy conversion, previous research indicates that NCM-622 is one of the best compositions in the field of EV application than others compositions (Kim, 2012, Wu et al., 2011). Several methods have been used in previous studies to synthesize NCM 622, such as sol-gel (Cao et

al., 2016), coprecipitation (Yang et al., 2014, Zheng et al., 2015), hydrothermal (Huang et al., 2022, Wang et al., 2016, Widiyandari et al., 2019), and solid-state method (Rahmawati et al., 2020). Among them, solid-state and hydrothermal methods are more applicable in large-scale industries.

Solid-state has the advantage of synthesizing cathode materials on a large scale because it is very simple regarding equipment requirements and the manufacturing process (Pan et al., 2013, Toprakci et al., 2010). Moreover, the hydrothermal process has the advantage of getting high single-crystalline of cathode materials (Huang et al., 2022).

In this work, a modified solid-state method for the preparation of NCM 622 cathode materials has been proposed and compared with the hydrothermal process. The structure, morphology, and electrochemical properties have been compared with the NCM cathode materials synthesized by the hydrothermal method.

EXPERIMENTAL

Materials and Methods

Nickel (II) sulfate hexahydrate ($NiSO_4.6H_2O$, Merck 99%), cobalt (II) sulfate heptahydrate ($CoSO_4.7H_2O$, Merck 99%), and manganese (II) sulfate monohydrate ($MnSO_4.H_2O$, Merck 99%) were used as the initial precursors. Each precursor was dissolved in water obtaining a concentration of 0.3 M and mixed with 0.3 M sodium carbonate (Na_2CO_3) to ion exchange of SO_4^{2-} to CO_3^{2-} to get metal carbonate and remove sulfur from the material, which can be impurity on NCM 622. Furthermore, this metal carbonate material is used in the NCM-622 synthesis process using various methods described below.

Hydrothermal

The metal carbonate material (Ni: Co: Mn = 0.6: 0.2: 0.2) was added to the oxalic acid solution as a chelating agent and LiOH with 5% excess as Li source with a mole ratio of metal carbonate: oxalic acid: LiOH is 1: 1: 1.05, then stirred at 400 rpm for 4 hours. After that, the solution was put into the autoclave and heated at 180°C for 20 h. Next, the solution was dried using an oven at 80°C for 12 h. The obtained powder was sintered under an air atmosphere initially at 450°C for 5 hours, followed by increasing the temperature to 850°C and kept for 16 hours.

Solid-State Reaction (SSR)

The metal carbonate material (Ni: Co: Mn = 0.6: 0.2: 0.2) was mixed with oxalic acid with a mole ratio of 1: 1 and then put into a planetary ball mill, wetted with ethanol to ensure the contact of powder materials for 6 hours with 1200 rpm. Then, LiOH with an excess of 5% was added to the mixed materials into a planetary ball mill and continued milled for 4 hours. After finishing the milling process, the mixture was transferred into the oven for drying at 80°C for 12 h. The obtained powder of the solid-state reaction then follows a similar sintering process as mentioned in the hydrothermal reaction.

Characterization and Electrochemical Test

The phase and crystal structure were identified using X-ray diffraction (XRD) with Cu-kα radiation (λ = 0.15406 nm). XRD data are obtained in the 2θ range from 10° to 80° using Rigaku Smartlab. Electrochemical testing was carried out using a coin-type cell (CR2025). Cyclic voltammetry (CV), charge/discharge, and Electrochemistry Impedance Spectroscopy (EIS) was carried out using WBCS 3000 Battery cycler and Hioki

3522. Cyclic voltammetry (CV) is measured from 2.5 to 4.3 V at a scan rate of 0.12 mV/s. The charge-discharge test was conducted using the constant current and constant voltage (CC-CV) mode with a voltage range of 2.0 – 4.3 V at 0.25 C.

RESULTS AND DISCUSSION

Figure 1 shows XRD patterns for each sample synthesized using different methods. It is clearly shown that the XRD peaks of (006/012) and (108/110) at 2θ of 38° and 2θ of 65° indicate well-defined layered structural characteristics for all samples (Chen et al., 2013, Luo et al., 2019). The results of the XRD data for all samples suggest that no impurity phase and additional peaks were formed after the synthesis process. The XRD peak of the solid-state reaction method is lower than hydrothermal, indicating the average grain size is reduced (Chao and Shuang-Yuan, 2020).

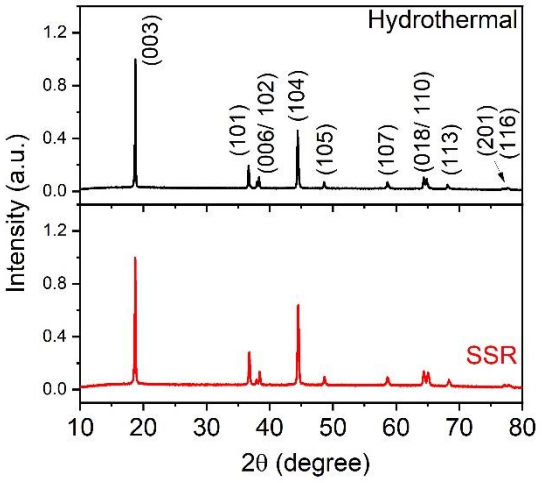

Fig. 1: The powder XRD pattern of synthesized NCM-622 by hydrothermal and solid-state (SSR) reaction method.

Table 1 shows the full width at half maximum (FWHM) of the samples. From the calculation of FWHM, solid-state reaction exhibits a higher FHWM value, leading to smaller crystallite size. The smaller crystallite size positively impacts lithium diffusion, electrolyte dispersion, and electrochemical performance (Bishnoi et al., 2017, Domi et al., 2019).

The other parameter is the intensity ratio (003) and (104) ($I_{(003)}$ / $I_{(104)}$), which can be used to estimate the cation mixing in the NCM materials (Peng et al., 2015, Yang et al., 2014, Zheng et al., 2015). The cation mixing phenomenon occurs because the Li^+ ions swap places with Ni^{2+} due to the ionic radius similarity between Li^+ (0.76 Å) and Ni^{2+} (0.69 Å). This mixing is undesirable because it can interfere with the electrochemical performance (Liu et al., 2014, Shim et al., 2014). Based on XRD data calculation, the crystallinity of NCM synthesized using hydrothermal, and solid-state reaction shows a comparable value on the degree of crystallinity, where hydrothermal and solid-state NCM crystallinity is at 91.8% and 86.7%, respectively. Furthermore, the I(003) / I(104) ratio (Table 1) of both samples exceeds 1.2, suggesting that low cation mixing can lead to better electrochemical performance (Peng et al., 2015, Yang et al., 2014, Zheng et al., 2015). Based on the two samples, peaks (006) / (012) and (018) / (110) have been formed, which indicates an increase in the layered crystal structure at NCM (Deng et al., 2010, Jan et al., 2014, Shi et al., 2013).

Several researchers use the c/a ratio as a parameter to indicate the layer structure of NCM (Wu et al., 2011, Zhu et al., 2014). The c /a ratio corresponds to the antisite disorder level of Ni^{2+} and Li^+. From Table 1, the solid-state reaction method shows a higher c/a ratio, incorporating better crystal ordering and lower antisite disordering of Ni^{2+} and Li^+. In their result, Zhu, et al explained that higher

c/a in NCM synthesized using molten salt synthesis is beneficial for a better intercalation process (Zhu et al., 2014).

Table 1. Parameter derived from XRD patterns

Sample	FWHM (003)	$I_{(003)}$ / $I_{(104)}$	c/a	Crystallinity (%)
Hydro-thermal	0.1158	1.49	4.94	91.8
SSR	0.1448	1.21	4.96	86.7

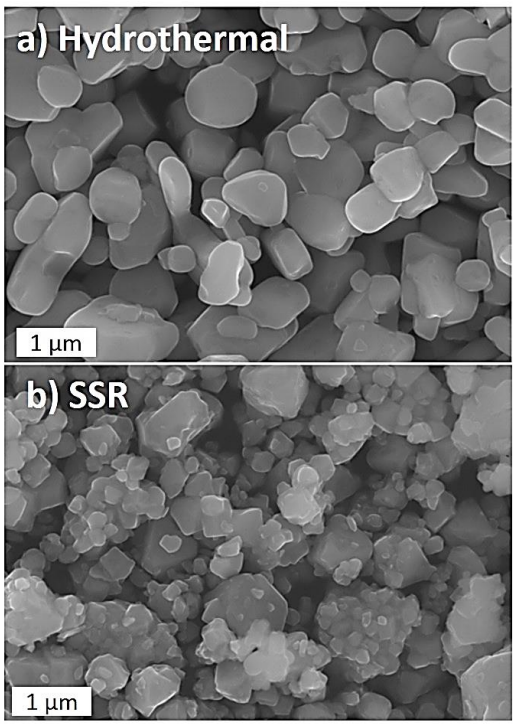

Fig. 2: SEM image of NCM-622 synthesized by a) Hydrothermal and b) Solid-state reaction methods

SEM was analyzed to understand the influence of the synthesis method on the surface morphology of both samples. Figure 2 shows SEM images captured from both samples have different morphology. The sample prepared using the hydrothermal method exhibits a bigger particle size and smooth surface. Meanwhile, the sample prepared using solid-state reaction shows smaller agglomeration of particles. This morphology agrees well with the XRD result where the grain size of solid-state NCM has a smaller size than hydrothermal one. The agglomeration of the smaller particle may increase the active surface area. Large surface area facilitates lithium movement during battery operation and enhances electrochemical performance (Ma and Tan, 2020, Trevisanello et al., 2021).

Figure 3 shows the cyclic voltammetry (CV) curve for each sample in the voltage range of 2.5 - 4.3 V at a scan rate of 0.12 mV/s. The redox peaks formed in all samples were between 3.6-4.0 V, corresponding to the Ni^{2+}/Ni^{4+} redox reaction in the NCM structure. In the voltage range of 3.2 V, the oxidation curve of Mn^{3+}/Mn^{4+} is not observed, indicating the absence of Mn^{3+}/Mn^{4+} redox reaction (Chong et al., 2016). Due to the inactive oxidation state of Mn^{4+}, it can be expected that the metal oxide lattice is quite stable.

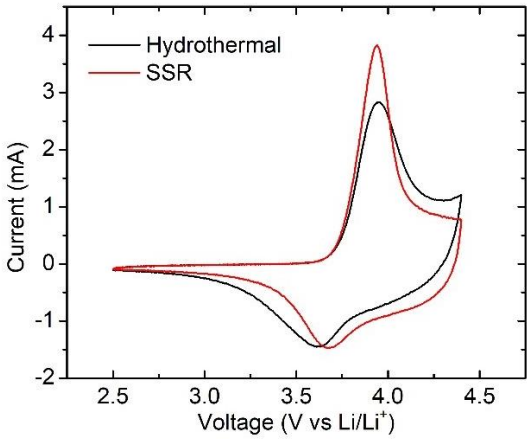

Fig. 3: Cyclic voltammetry profiles of samples synthesized by hydrothermal and solid-state reaction (SSR) method at scan rate 0.12 mV/s.

In the CV curve, the anodic and cathodic peak potential intervals indicate the diffusion of lithium ions and the transfer of electrons between the electrodes, respectively. The

solid-state reaction approach has a lower ΔE than the hydrothermal one for both NCM samples, as shown in Table 2. Lower ΔE indicates a greater reversibility rate owing to the ease of lithium-ion intercalation and deintercalation, which is essential for BEV applications (Habibi et al., 2018).

Table 2. Initial charge/discharge capacity values for different samples.

Sample	$E_{oxidation}$ (V)	$E_{reduction}$ (V)	ΔE
Hydro-thermal	3.95	3.59	0.36
SSR	3.93	3.68	0.25

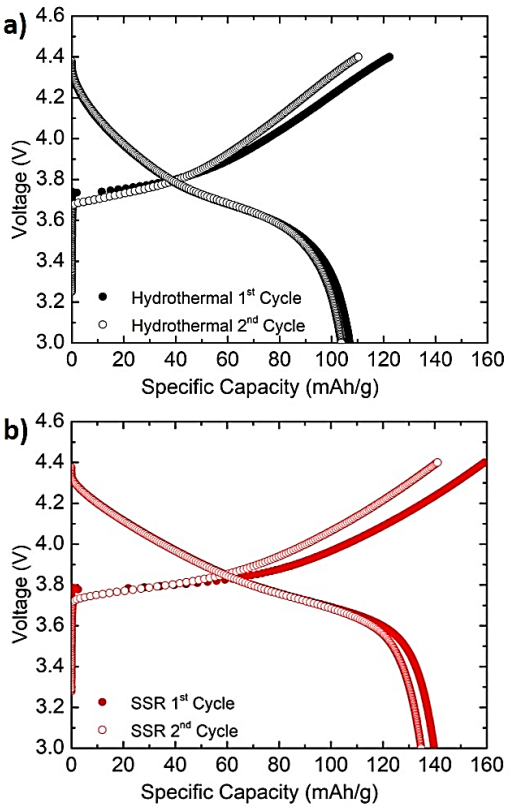

Fig. 4: Charge discharge performance of a) Hydrothermal and b) Solid-state reaction NCM-622 at 1st and 2nd cycle at 0.25 C.

Figure 4 shows the charge-discharge curve of both samples at the first and second cycles. Each sample shows a smooth and regular shape curve that indicates the structure stability of prepared layered NCM. Both samples show decreasing capacity from the first to the second cycle. The initial charge and discharge capacity of both samples are 122.32 and 106.98 mAh/g (87.44% coulombic efficiency) and 159.12 and 139.74 mAh/g (87.55% coulombic efficiency) for hydrothermal and solid-state reaction, respectively. The initial discharge capacity of hydrothermal is lower than solid-state NCM. Lowering capacity on the 2nd cycle is caused by irreversible electrolyte oxidation for Solid Electrolyte Interphase (SEI) (Kasnatscheew et al., 2016, Tan et al., 2015).

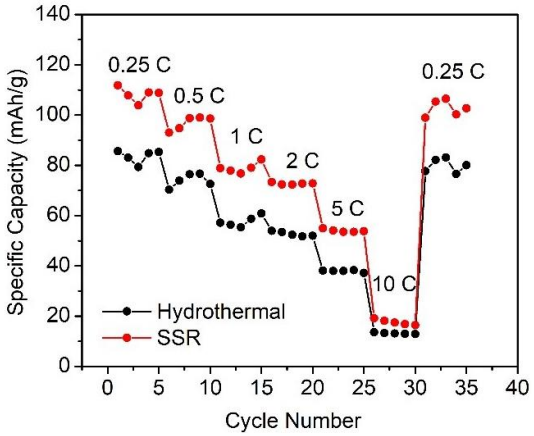

Fig. 5: Rate performance of NCM-622 synthesized by Hydrothermal and solid-state reaction (SSR) at 0.25 C to 10 C at the voltage range 3 – 4.3 volt.

Figure 5 illustrates the rate performance of the two samples at 3.0-4.3 Volt. The specific capacity of all samples decreases at an increasing rate. The NCM synthesized using hydrothermal methods shows lower rate performance than solid-state reaction. The performance enhancement of solid-state reaction may be due to better ionic conductivity, leading to better Li-ion diffusion between the electrode and the electrolyte

interface (Wang et al., 2019). After several cycles at different C rates, the specific capacity difference between the first and final cycles is slightly reduced in the two samples. These phenomena indicate that these two samples have good cycle ability and less irreversible reaction during the charge and discharge process.

Figure 6 represents the Electrochemical Impedance Spectroscopy (EIS) test results in which all samples provide a Nyquist plot graph after the battery conduct charge and discharge at different scan rate conditions. Nyquist plots consist of semi-circles from low-to-high frequency and additional straight lines. The semi-circles at medium to the high-frequency region are addressed to the charge transfer resistance (R_{ct}). On the other hand, a straight line with a gradient of ±45° corresponds to the Warburg impedance (Subhan et al., 2019). The Warburg impedance is a parameter associated with the lithium diffusion (D_{Li}) behavior of the electrode. The resistance and the lithium diffusion act as important roles in analyzing the battery performance.

The values of charge-transfer resistance (Rct), conductivity, and lithium-ion diffusivity (DLi) parameters were obtained based on the two sample fittings. Each impedance spectrum is fitted well with the suggested equivalent circuit model. Based on the fitted EIS data, the R_{ct} for hydrothermal and the solid-state reaction NCM is 307.747 and 228.019 Ω, respectively. The smaller the R_{ct}, the higher the conductivity so that the material is easier to conduct electric current (Subhan et al., 2019). Solid–state reaction NCM shows lower R_{ct} than hydrothermal NCM, indicating that the charge transfer at the electrode and electrolyte on the battery system greatly improved electrochemical performance. Regarding the calculation related to the lithium-ion diffusivity (D_{Li}), Hydrothermal and solid-state reaction NCM have 2.548 x 10^{-18} (cm^2/s) and 3.528 x 10^{-18} (cm^2/s), respectively. A lower c/a ratio of the solid-state reaction NCM could maintain the lithium-ion diffusivity (D_{Li}) through the NCM electrode.

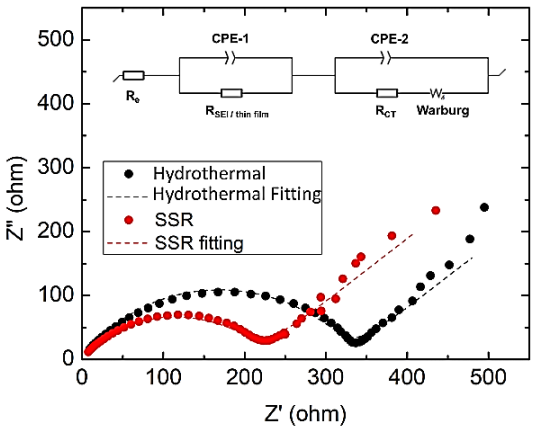

Fig. 6: Electrochemical Impedance Spectroscopy profiles of the as-synthesized NCM-622 samples by different synthesis methods.

CONCLUSIONS

NCM-622 has been synthesized using a hydrothermal and solid-state reaction. The hydrothermal method is a promising candidate for preparing cathode materials with high crystallinity and uniform structure. On the other side, large-scale cathode production demands a consistent and simple process. This paper observed that the preparation result using hydrothermal and solid-state reactions has a similar result. Regarding the electrochemical performance, NCM derived from the solid-state reaction method performs better than hydrothermal NCM due to its low charge transfer resistance followed by a higher ion diffusion rate. When tested in a lithium-ion battery, the 25.9% lower Rct and 38.5% higher diffusivity improve performance. Such performance is

likely related to the smaller particle of the as-synthesized NCM by the solid-state reaction method.

ACKNOWLEDGEMENT

The author is grateful for the financial support from the Downstream Research and Technology Innovation, Research and Technology Innovation, PT Pertamina (Persero).

REFERENCES

Andre, D., Kim, S.-J., Lamp, P., Lux, S.F., Maglia, F., Paschos, O., and Stiaszny, B., 2015. "Future generations of cathode materials: an automotive industry perspective." *J. Mater. Chem. A, 3*, 6709–6732. https://doi.org/10.1039/C5TA00361J

Bak, S.-M., Hu, E., Zhou, Y., Yu, X., Senanayake, S.D., Cho, S.-J., Kim, K.-B., Chung, K.Y., Yang, X.-Q., and Nam, K.-W., 2014. "Structural Changes and Thermal Stability of Charged LiNixMnyCozO2 Cathode Materials Studied by Combined In Situ Time-Resolved XRD and Mass Spectroscopy." *ACS Appl. Mater. Interfaces 6*, 22594–22601. https://doi.org/10.1021/am506712c

Bishnoi, A., Kumar, S., and Joshi, N., 2017. "Chapter 9 - Wide-Angle X-ray Diffraction (WXRD): Technique for Characterization of Nanomaterials and Polymer Nanocomposites," in: Thomas, S., Thomas, R., Zachariah, A.K., Mishra, R.K.B.T.-M.M. in N.C. (Eds.), Micro and Nano Technologies. Elsevier, pp. 313–337. https://doi.org/10.1016/B978-0-323-46141-2.00009-2

Cao, Xiaoyu, Zhao, Y., Zhu, L., Xie, L., Cao, Xiaoli, Xiong, S., and Wang, C., 2016. "Synthesis and Characterization of LiNi1/3Co1/3Mn1/3O2 as Cathode Materials for Li-Ion Batteries via an Efficacious Sol- Gel Method." *Int. J. Electrochem. Sci., 11*, 5267–5278. https://doi.org/10.20964/2016.06.93

Chao, M., and Shuang-Yuan, T., 2020. "Hydrothermal Synthesis and Electrochemical Performance of Micro-spherical LiNi1/3Co1/3Mn1/3O2 Cathode Material." *Int. J. Electrochem. Sci., 15*, 9392–9401. https://doi.org/10.20964/2020.09.53

Chen, C.-L., Chiu, K.-F., Leu, H.J., and Chen, C.C., 2013. "Iron Hexacyanoferrate Based Compound Modified LiMn2O4 Cathodes for Lithium Ion Batteries." *J. Electrochem. Soc., 160*, A3126. https://doi.org/10.1149/2.020305jes

Chong, S., Liu, Y., Yan, W., and Chen, Y., 2016. "Effect of valence states of Ni and Mn on the structural and electrochemical properties of Li1.2NixMn0.8−xO2 cathode materials for lithium-ion batteries." *RSC Adv. 6*, 53662–53668. https://doi.org/10.1039/C6RA09454F

Deng, C., Zhang, S., Fu, B.L., Yang, S.Y., and Ma, L., 2010. "Synthetic optimization of nanostructured Li[Ni1/3Mn1/3Co1/3]O2 cathode material prepared by hydroxide coprecipitation at 273K." *J. Alloys Compd., 496*, 521–527. https://doi.org/10.1016/j.jallcom.2010.02.094

Domi, Y., Usui, H., Sugimoto, K., and Sakaguchi, H., 2019. "Effect of Silicon Crystallite Size on Its Electrochemical Performance for Lithium-Ion Batteries." *Energy Technol., 7*, 1800946. https://doi.org/https://doi.org/10.1002/ente.201800946

Geldasa, F.T., Kebede, M.A., Shura, M.W., and

Hone, F.G., 2022. "Identifying surface degradation, mechanical failure, and thermal instability phenomena of high energy density Ni-rich NCM cathode materials for lithium-ion batteries: a review." *RSC Adv., 12*, 5891–5909. https://doi.org/10.1039/D1RA08401A

Habibi, A., Jalaly, M., Rahmanifard, R., and Ghorbanzadeh, M., 2018. "The effect of calcination conditions on the crystal growth and battery performance of nanocrystalline Li(Ni1/3Co1/3Mn1/3)O2 as a cathode material for Li-ion batteries." *New J. Chem., 42*, 19026–19033. https://doi.org/10.1039/C8NJ05007D

Huang, X., Zhang, P., Liu, Z., Ma, B., Zhou, Y., and Tian, X., 2022. "Fluorine Doping Induced Crystal Space Change and Performance Improvement of Single Crystalline LiNi0.6Co0.2Mn0.2O2 Layered Cathode Materials." *ChemElectroChem, 9*, e202100756. https://doi.org/https://doi.org/10.1002/celc.202100756

Jan, S.S., Nurgul, S., Shi, X., Xia, H., and Pang, H., 2014. "Improvement of electrochemical performance of LiNi0.8Co0.1Mn0.1O2 cathode material by graphene nanosheets modification." *Electrochim. Acta, 149*, 86–93. https://doi.org/10.1016/j.electacta.2014.10.093

Julien, C.M., Mauger, A., Zaghib, K., and Groult, H., 2014. "Comparative issues of cathode materials for Li-ion batteries." *Inorganics*, *2*, 132–154. https://doi.org/10.3390/inorganics2010132

Kasnatscheew, J., Evertz, M., Streipert, B., Wagner, R., Klöpsch, R., Vortmann, B., Hahn, H., Nowak, S., Amereller, M., Gentschev, A.-C., Lamp, P., and Winter, M., 2016. "The truth about the 1st cycle Coulombic efficiency of LiNi1/3Co1/3Mn1/3O2 (NCM) cathodes." *Phys. Chem. Chem. Phys., 18*, 3956–3965. https://doi.org/10.1039/C5CP07718D

Kim, Y., 2012. "Lithium Nickel Cobalt Manganese Oxide Synthesized Using Alkali Chloride Flux: Morphology and Performance As a Cathode Material for Lithium Ion Batteries." *ACS Appl. Mater. Interfaces, 4*, 2329–2333. https://doi.org/10.1021/am300386j

Konishi, H., Yoshikawa, M., and Hirano, T., 2013. "The effect of thermal stability for high-Ni-content layer-structured cathode materials, LiNi0.8Mn0.1−xCo0.1MoxO2 (x = 0, 0.02, 0.04)." *J. Power Sources, 244*, 23–28. https://doi.org/10.1016/j.jpowsour.2013.05.004

Konishi, H., Yuasa, T., and Yoshikawa, M., 2011. "Thermal stability of Li1−yNixMn(1−x)/2Co(1−x)/2O2 layer-structured cathode materials used in Li-Ion batteries." *J. Power Sources, 196*, 6884–6888. https://doi.org/10.1016/j.jpowsour.2011.01.016

Li, T., Yuan, X.-Z., Zhang, L., Song, D., Shi, K., and Bock, C., 2020. "Degradation Mechanisms and Mitigation Strategies of Nickel-Rich NMC-Based Lithium-Ion Batteries." *Electrochem. Energy Rev., 3*, 43–80. https://doi.org/10.1007/s41918-019-00053-3

Liu, S., Xiong, L., and He, C., 2014. "Long cycle life lithium ion battery with lithium nickel cobalt manganese oxide (NCM) cathode." *J. Power Sources, 261*, 285–291. https://doi.org/10.1016/j.jpowsour.2014.03.083

Luo, B., Jiang, B., Peng, P., Huang, J., Chen, J., Li, M., Chu, L., and Li, Y., 2019. "Improving

the electrochemical performance of LiNi1/3Co1/3Mn1/3O2 cathode material via tungsten modification." *Electrochim. Acta, 297*, 398–405. https://doi.org/10.1016/j.electacta.2018.11.202

Ma, C., and Tan, S.-Y., 2020. "Hydrothermal Synthesis and Electrochemical Performance of Micro-spherical LiNi1/3Co1/3Mn1/3O2 Cathode Material." *Int. J. Electrochem. Sci., 15*, 9392–9401. https://doi.org/10.20964/2020.09.53

Myung, S.-T., Maglia, F., Park, K.-J., Yoon, C.S., Lamp, P., Kim, S.-J., and Sun, Y.-K., 2017. "Nickel-Rich Layered Cathode Materials for Automotive Lithium-Ion Batteries: Achievements and Perspectives." *ACS Energy Lett., 2*, 196–223. https://doi.org/10.1021/acsenergylett.6b00594

Or, T., Gourley, S.W.D., Kaliyappan, K., Yu, A., and Chen, Z., 2020. "Recycling of mixed cathode lithium-ion batteries for electric vehicles: Current status and future outlook." *Carbon Energy, 2*, 6–43. https://doi.org/https://doi.org/10.1002/cey2.29

Pan, C., Banks, C.E., Song, W., Wang, C., Chen, Q., and Ji, X., 2013. "Recent development of LiNixCoyMnzO2: Impact of micro/nano structures for imparting improvements in lithium batteries." *Trans. Nonferrous Met. Soc. China, 23*, 108–119. https://doi.org/10.1016/S1003-6326(13)62436-X

Park, O.K., Cho, Y., Lee, S., Yoo, H.-C., Song, H.-K., and Cho, J., 2011. "Who will drive electric vehicles, olivine or spinel?" *Energy Environ. Sci., 4*, 1621–1633. https://doi.org/10.1039/C0EE00559B

Peng, L., Zhu, Y., Khakoo, U., Chen, D., and Yu, G., 2015. "Self-assembled LiNi1/3Co1/3Mn1/3O2 nanosheet cathodes with tunable rate capability." *Nano Energy, 17*, 36–42. https://doi.org/10.1016/j.nanoen.2015.07.031

Rahmawati, M., Purwanto, A., Widiyandari, H., Paramitha, T., Nizam, M., Dyartanti, E.R., Muzayahna, S.U., and Yudha, C.S., 2020. "Synthesis of NMC 111 via urea assisted solid state method." *AIP Conf. Proc., 2197*, 50007. https://doi.org/10.1063/1.5140919

Seungbum, H., Yoon, B., Lim, H., Seo, H.-K., Lee, C.-R., and Seo, I., 2022. "Photo-Charging of Li(Ni0.65Co0.15Mn0.20)O2 Lithium-Ion Battery Using Silicon Solar Cells." *Materials (Basel)., 15*. https://doi.org/10.3390/ma15082913

Shi, S.J., Tu, J.P., Tang, Y.Y., Zhang, Y.Q., Liu, X.Y., Wang, X.L., and Gu, C.D., 2013. "Enhanced electrochemical performance of LiF-modified LiNi1/3Co1/3Mn1/3O2 cathode materials for Li-ion batteries." *J. Power Sources, 225*, 338–346. https://doi.org/10.1016/j.jpowsour.2012.10.065

Shim, J.-H., Kim, C.-Y., Cho, S.-W., Missiul, A., Kim, J.-K., Ahn, Y.J., and Lee, S., 2014. "Effects of heat-treatment atmosphere on electrochemical performances of Ni-rich mixed-metal oxide (LiNi0.80Co0.15Mn0.05O2) as a cathode material for lithium ion battery." *Electrochim. Acta, 138*, 15–21. https://doi.org/10.1016/j.electacta.2014.06.079

Subhan, A., Oemry, F., Khusna, S.N., and Hastuti, E., 2019. "Effects of activated carbon treatment on Li4Ti5O12 anode material synthesis for lithium-ion

batteries." *Ionics (Kiel)., 25*, 1025–1034. https://doi.org/10.1007/s11581-018-2633-0

Tan, S., Wang, L., Bian, L., Xu, J., Ren, W., Hu, P., and Chang, A., 2015. "Highly enhanced low temperature discharge capacity of LiNi1/3Co1/3Mn1/3O2 with lithium boron oxide glass modification." *J. Power Sources, 277*, 139–146. https://doi.org/10.1016/j.jpowsour.2014.11.149

Toprakci, O., Toprakci, H.A.K., Ji, L., and Zhang, X., 2010. "Fabrication and Electrochemical Characteristics of $LiFePO_4$ Powders for Lithium-Ion Batteries." *KONA Powder Part. J., 28*, 50–73. https://doi.org/10.14356/kona.2010008

Trevisanello, E., Ruess, R., Conforto, G., Richter, F.H., and Janek, J., 2021. "Polycrystalline and Single Crystalline NCM Cathode Materials—Quantifying Particle Cracking, Active Surface Area, and Lithium Diffusion." *Adv. Energy Mater., 11*, 2003400. https://doi.org/https://doi.org/10.1002/aenm.202003400

Wang, L., Wang, Y., Yang, Xiaheng, Wang, J., Yang, Xiduo, and Tang, J., 2019. "Excellent cyclability of P2-type Na–Co–Mn–Si–O cathode material for high-rate sodium-ion batteries." *J. Mater. Sci., 54*, 12723–12736. https://doi.org/10.1007/s10853-019-03807-y

Wang, L., Wu, B., Mu, D., Liu, X., Peng, Y., Xu, H., Liu, Q., Gai, L., and Wu, F., 2016. "Single-crystal LiNi0.6Co0.2Mn0.2O2 as high performance cathode materials for Li-ion batteries." *J. Alloys Compd., 674*, 360–367. https://doi.org/10.1016/j.jallcom.2016.03.061

Widiyandari, H., Sukmawati, A.N., Sutanto, H., Yudha, C., and Purwanto, A., 2019. "Synthesis of $LiNi_{0.8}Mn_{0.1}Co_{0.1}O_2$ cathode material by hydrothermal method for high energy density lithium ion battery." *J. Phys. Conf. Ser., 1153*, 12074. https://doi.org/10.1088/1742-6596/1153/1/012074

Wu, L., Nam, K.-W., Wang, X., Zhou, Y., Zheng, J.-C., Yang, X.-Q., and Zhu, Y., 2011. "Structural Origin of Overcharge-Induced Thermal Instability of Ni-Containing Layered-Cathodes for High-Energy-Density Lithium Batteries." *Chem. Mater., 23*, 3953–3960. https://doi.org/10.1021/cm201452q

Wu, Y., Li, M., Wahyudi, W., Sheng, G., Miao, X., Anthopoulos, T.D., Huang, K.-W., Li, Y., and Lai, Z., 2019. "Performance and Stability Improvement of Layered NCM Lithium-Ion Batteries at High Voltage by a Microporous Al2O3 Sol-Gel Coating." *ACS omega*., 4 (9), 13972–13980 https://doi.org/10.1021/acsomega.9b01706

Yang, Z., Lu, J., Bian, D., Zhang, W., Yang, X., Xia, J., Chen, G., Gu, H., and Ma, G., 2014. "Stepwise coprecipitation to synthesize LiNi1/3Co1/3Mn1/3O2 one-dimensional hierarchical structure for lithium ion batteries." *J. Power Sources, 272*, 144–151. https://doi.org/10.1016/j.jpowsour.2014.08.052

Zheng, X., Li, X., Huang, Z., Zhang, B., Wang, Z., Guo, H., and Yang, Z., 2015. "Enhanced electrochemical performance of LiNi0.6Co0.2Mn0.2O2 cathode materials by ultrasonic-assisted coprecipitation method." *J. Alloys Compd., 644*, 607–614. https://doi.org/10.1016/j.jallcom.2015.04.173

Zhu, H., Li, J., Chen, Z., Li, Q., Xie, T., Li, L., and Lai, Y., 2014. "Molten salt synthesis and

electrochemical properties of LiNi1/3Co1/3Mn1/3O2 cathode materials." *Synth. Met., 187*, 123–129. https://doi.org/10.1016/j.synthmet.2013.10.032.